Technical Correspondence

Situation Awareness Inferred From Posture Transition and Location: Derived From Smartphone and Smart home Sensors

Shumei Zhang, Paul McCullagh, Huiru Zheng, and Chris Nugent

Abstract—Situation awareness may be inferred from user context such as body posture transition and location data. Smartphones and smart homes incorporate sensors that can record this information without significant inconvenience to the user. Algorithms were developed to classify activity postures to infer current situations; and to measure user's physical location, in order to provide context that assists such interpretation. Location was detected using a subarea-mapping algorithm; activity classification was performed using a hierarchical algorithm with backward reasoning; and falls were detected using fused multiple contexts (current posture, posture transition, location, and heart rate) based on two models: "certain fall" and "possible fall." The approaches were evaluated on nine volunteers using a smartphone, which provided accelerometer and orientation data, and a radio frequency identification network deployed at an indoor environment. Experimental results illustrated falls detection sensitivity of 94.7% and specificity of 85.7%. By providing appropriate context the robustness of situation recognition algorithms can be enhanced.

Index Terms—Assisted living, body sensor networks (BSNs), context awareness, wearable computers.

I. INTRODUCTION

Many studies have utilized intelligent environments to assist elderly or vulnerable people to live independently at home and to potentially maintain their quality of life. One goal of smart homes is to monitor lifestyle (such as activities and locations) of the occupant in order to promote autonomy and independent living and to increase feelings of security and safety. Sensing technology of various forms has been employed to track the activities and locations within the home environment. Derived information can be used as input to control domestic devices such as lighting, heater, television, and cooker based on a user's current activity and location [1]. Radio frequency (RF) identification (RFID), body sensor networks (BSNs), and wireless sensor networks (WSNs) are complementary technologies used in this research environment. RFID can identify and track the location of tagged occupants, BSNs can record movement, orientation, and biosignals, and WSNs can discover and record attributes within and about the environment

(e.g., temperature, status of doors and windows). All components have the capacity to communicate wirelessly and be connected as an "Internet of Things," providing an associated "big data" resource, usually of unstructured data yielding a potential interpretation and understanding problem for the researcher. If this problem can be successfully addressed, then knowledge regarding identity, activity, location, and environmental conditions can be derived by integrating data from RFID with BSNs and WSNs. This vision drives an area of significant research effort, which may be classified as "situation awareness" leading to situation recognition. The research poses challenges for communications infrastructure, connected health monitoring, and acceptance of technology by the user; much of which relies upon computing advances.

The World Health Organization estimated that 424 000 fatal falls occur each year, making falls a leading cause of accidental deaths. Elderly people over 70 years have the highest risk of fatal falls, more than 32% of older persons have experienced a fall at least once a year with 24% encountering serious injuries [2], [3]. Approximately 3% of people who experience a fall remain on the ground or floor for more than 20 min prior to receiving assistance [4]. A serious fall decreases an older person's self-confidence and motivation for independence and even for remaining in his/her own home. Therefore, a situation awareness system can assist frail people living at home and potentially sustain a good quality of life for longer.

The aim of this work is to combine smartphone and smart home technology to provide context on posture transition and location. This research developed a monitoring system to identify users' activities, locations, and hence to infer users' current situations; should an abnormal situation be classified then an alert may be delivered to the user or to a guardian, if necessary. In particular, we attempt to detect falls and posture transitions using BSNs and an RFID-enabled smart home.

The paper is organized as follows. Related work is discussed in Section II, and methodologies for the system configuration and current situation detection algorithms are described in Section III. The experiments undertaken and results obtained are presented in Section IV. Section V focuses on discussion, limitations of the approach, and future work.

II. RELATED WORK

A. Detection of Falls

Falls may be detected by using devices such as environment-embedded sensors and wearable sensors. Wireless optical cameras can be embedded in a tracking environment [5]; however, they can only monitor fixed places and there can be privacy protection issues to resolve for smart home occupants [6]. Depth-based sensors such as Kinect [7] do not reproduce images and can overcome acceptance issues. Such devices are feasible and maybe useful at high-risk

locations for falls. Wearable sensors comprising gyroscopes, tilt sensors, and accelerometers allow users to be monitored within and outside of their home environment. Such sensors can be integrated into existing community-based alarm and emergency systems [8]. For example, the MCT-241MD PERS [9] is a commercial product that detects falls. A built-in tilt sensor and a manual emergency alert button can trigger a call to a remote monitoring station for help, when tilts of more than 60° lasting more than a minute are detected.

Kangas *et al.* [10] investigated acceleration of falls from sensors attached to the waist, wrist, and head, and demonstrated that measurements from the waist and head were more useful for fall detection. Lindemann *et al.* [11] quantified fall detection using two head-worn accelerometers that offer sensitive impact detection for heavy falls based on three predefined thresholds. Smartphone sensors also face usability and acceptance issues, particularly if required to be worn in a predetermined position (e.g., waist) and orientation [12]. Whilst they may not yet provide a "real living" solution, a system based on a smartphone does not suffer the same obstacles of setup time and stigmatization as dedicated laboratory sensors systems such as XSENS [13]. Hence, it is worthwhile determining whether using a phone can be beneficial for inferring "situations." Their pervasive nature, computational power, connectedness, and multifunction capability are clearly advantageous as the phone can deliver real-time feedback and/or alert messages across the full range of communication platforms (telephone, internet, and social media).

Methods that use only the accelerometer with some empirical threshold can lead to many false positives from other "fall-like" activities such as sitting down quickly and jumping, which feature a large change in vertical acceleration. In order to improve the reliability of fall detection, studies combined accelerometers with other sensors. Bianchi *et al.* [14] integrated an accelerometer with a barometric pressure sensor into a wearable device, and demonstrated that fall detection accuracy improved in comparison to using accelerometer data alone (96.9% versus 85.3%). Li *et al.* [15] combined two accelerometers with gyroscopes on the chest and thigh, respectively, and concluded that fall detection accuracy improved. Machine learning techniques have also been used to improve falls detection and recognition [16], [17].

B. Location Tracking

Location tracking systems are varied in their accuracy, range, and infrastructure costs. The challenges are how to achieve more accurate fine-grained subarea-position estimation while minimizing equipment costs. For localization outdoors, the global positioning system (GPS) works well in most environments. However, the signal from satellites cannot penetrate most buildings, so GPS cannot be used reliably in indoor locations.

Schemes envisioned for indoor localization are mostly based on machine vision, laser range-finding, or cell network localization [18]. The "Ubiquitous Home" [19] was equipped with a variety of sensors, such as cameras, microphones, floor pressure sensors, RFID, and accelerometers to monitor human activities and their location.

There are many challenges associated with RFID deployment in a smart home environment. For example, deployment should consider the facilities arrangement, to deal with missing data caused by interfering, absorbing, or distorting factors, and to ensure best coverage using the minimum number of readers. RFID reader deployment can be assessed by practice in experimental trials or by calculation using mathematical algorithms [20], [21]. The practical approach arranges the readers using
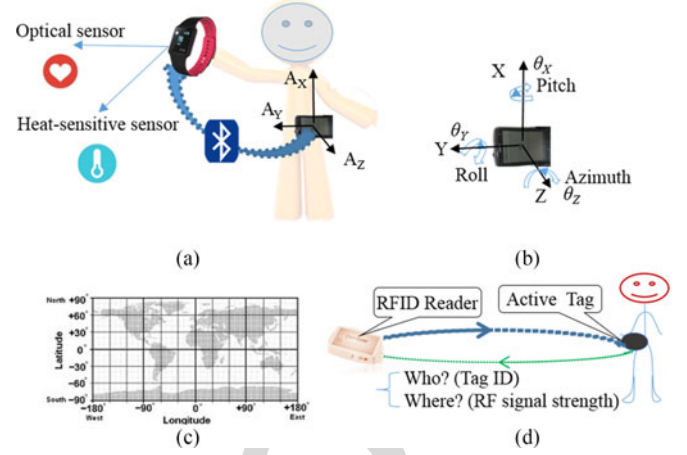

Fig. 1. System configuration; datasets acquired from the phone's sensors, smartwatch's sensors, and RFID networks at indoor: (a) acceleration with heart rate, (b) orientation angles, (c) geocoordinate (latitude, longitude), and (d) RFID networks (ID, R_{SS}).

personal experience [22]. The mathematical approach formulates the sensor deployment as a search algorithm. Algorithms investigated include generic search and simulated annealing [23]. Reza and Geok [24] introduced a geometric grid-covering algorithm for reader deployment inside buildings and achieved an average accuracy of 0.6 m.

RFID localization methods can be classified into two categories: 1) position is estimated by using distances calculated based on a signal propagation model; 2) position is estimated by using RF signal strength (R_{SS}) directly. In 1), the position of a target subject is triangulated in the form of coordinates (distances between the tag and each of the fixed readers), based on an empirical RF propagation model [25], [26]. In 2), the R_{SS} values are mapped onto a defined physical area based on a number of reference nodes using their known positions. Using this method, it is possible to reduce the errors caused by the translation from R_{SS} to distance, as it avoids use of the RF signal propagation model. Learning approaches have been based upon the k-NN algorithm [27], [28] or a kernel-based algorithm [29].

The research discussed in this paper detects falls based on integrated multiple contexts, e.g., activity postures, location, and heart rate.

III. METHODOLOGY

We developed and subsequently evaluated a situation-aware system using a smartphone, which could infer activity from a users' posture, posture transition, and their current position. Detection of falls provides an exemplar but other activities can be inferred.

A. System Configuration

The hardware comprised an HTC802w smartphone connected with a HiCling smartwatch and an RFID network. The system configuration is shown in Fig. 1. The phone connects with the watch via Bluetooth, and communicates with the RFID reader via WiFi. Feedback was delivered via the phone using voice and text messages.

The phone's processor operated at 1.7 GHz, the memory capacity was 2 GB with an additional 32 GB memory card and the operating system was Android 4.4.3. The phone embedded ten types of sensors, but only GPS, 3-axis accelerometer, and the orientation sensors were used.

The phone was belt-worn on the left side of the waist in a horizontal orientation. In this case, the accelerometer coordinate system is that the
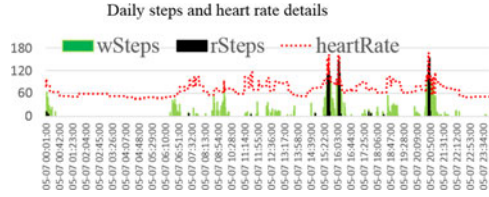
Fig. 2. Heart rate measurement compared to walk and run steps. The heart rate intensity zone can be used for physical activity intensity analysis.
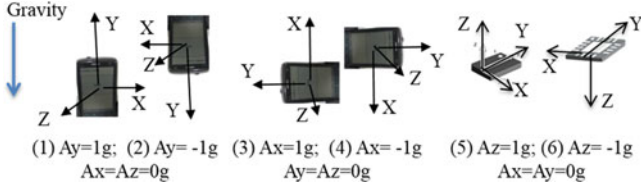

Fig. 3. Six 3-D coordinate systems based on the phone's orientation.

Fig. 4. Relationship between the body postures and maximum value of ($|Ax|$, $|Ay|$, $|Az|$).

TABLE I
BODY POSTURES WITH 3-D ROTATION ANGLES (θx, θy, θz)

Tilted angles (θ_X, θ_Y)		Body postures	Orientation angle θ_Z [0°, 360°]	Orientation
θ_X [−180°, 180°]	θ_Y [−90°, 90°]			
$\leq 0 + \theta_{caliX}$	$\geq 90 - \theta_{caliY}$	Upright	0 or 360	North
$\leq 0 + \theta_{caliX}$	$\leq 90 - \theta_{caliY}$	Tilted right	90	East
$\theta_{caliX} \leq |\theta_X| \leq 90$	$\leq 90 - \theta_{caliY}$	Tilted back	180	South
$\geq 180 - \theta_{caliX}$	$\geq 90 - \theta_{caliY}$	Tilted left	270	West

Here $\theta_{CaliX} = 10$, $\theta_{CaliY} = 20$ are empirical calibration values.

X-axis is vertical, the Y-axis is horizontal, and the Z-axis is orthogonal to the screen, as shown in Fig. 1(a). The phone's orientation can be monitored using the orientation sensor. This sensor provides three-dimensional (3-D) rotation angles along the three axes (*pitch, roll, azimuth*), denoted as (θ_X, θ_Y, θ_Z), as depicted in Fig. 1(b).

Fig. 2 shows a user's daily steps of walk and run as well as instantaneous heart rate, obtained from the smartwatch.

The smartwatch was embedded with optical sensor, 3-D accelerometer, captive skin touch sensor, and Bluetooth 4.0. The minute-based dataset accessed from the watch provides a parameter set (*t, wSteps, rSteps, heartrate, isWear*). The parameter isWear indicates whether the user has watch on, wSteps is walking steps, rSteps is run steps.

The outdoor localization is determined via GPS using the geocoordinate (latitude, longitude) as shown in Fig. 1(c). The indoor localization is recognized via a predeployed RFID network. The position (where?) is determined by received RF signal strength (R_{SS}); identity (who?) is provided by RFID tag ID, as shown in Fig. 1(d). The RFID reader/active tag frequency was 868 MHz, with a theoretical detection range of up to 8 m.

B. Data Acquisition

Five datasets: 3-D acceleration (*t, Ax, Ay, Az*), 3-D orientation angles (*t*, θ_X, θ_Y, θ_Z), vital signs signal (*t, heartrate, isWear*), geocoordinates (*t*, latitude, longitude), and RFID data series of (*t*, ID, R_{SS}) were obtained. Subsequently, the datasets were used for the evaluation of the posture classification, location recognition, and by further processing to infer fall detection.

1) Acceleration: For a tri-axis accelerometer, six 3-D coordinate systems are apparent (vertical axis is X, Y, or Z in upward or downward directions) according to the phone's orientation, as shown in Fig. 3 (1)–(6).

Fig. 3 illustrates the tri-axis directions determined by the phone's orientation. The absolute value of vertical acceleration is equal to the maximum stationary value among ($|A_x|$, $|A_y|$, $|A_z|$) as shown in the following equation:

$$|A_{\text{vertical}}| = \text{Max}\left(|A_x|, |A_y|, |A_z|\right). \quad (1)$$

Equation (1) declares that the vertical-axis acceleration depends on the orientation, so postures (such as lying) can be inferred according to the vertical-axis shifts among (Ax, Ay, Az), as shown in the acceleration patterns in Fig. 4.
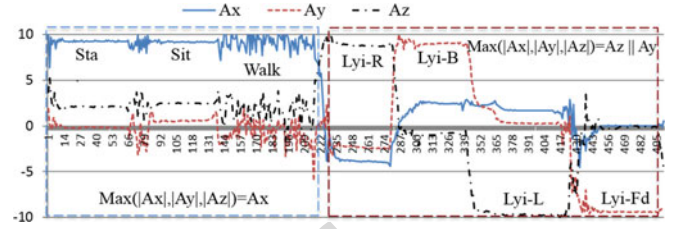
If the upper body posture is upright (stand, sit, or walk), then the maximum absolute acceleration is Ax, and the X-axis is vertical, since the phone has horizontal orientation. If the body posture is lying right, lying back, lying left, or lying face down, then the vertical axis is the Y- or Z-axis, so the maximum value of ($|Ax|$, $|Ay|$, $|Az|$) must be Ay or Az. In theory, one axis may indicate the influence of acceleration due to gravity (± 9.81 m/s^2) and the other two should be zero. In practice, orientation somewhat between states, transition in orientation, movement, and artifact impose relative noise making transitions less precise. Further details on methodology and heuristic classification rules to infer posture by accelerometry are provided in [30].

2) Orientation Angles: The orientation sensor provides 3-D rotation angles along the three axes (pitch, roll, azimuth) are denoted as (θ_X, θ_Y, θ_Z).

1) Pitch (θ_X), degrees of rotation around the X-axis, the range of values is [−180°, 180°], with positive values when the positive Z-axis moves toward the positive Y-axis.
2) Roll (θ_Y), degrees of rotation around the Y-axis, $−90° <= \theta_Y <= 90°$, with positive values when the positive Z-axis moves towards the positive X-axis.
3) Azimuth (θ_Z), degrees of rotation around the Z-axis, $\theta_Z = [0°, 360°]$. It is used to detect the compass direction. $\theta_Z = 0°$ or 360°, north; $\theta_Z = 180°$, south; $\theta_Z = 90°$, east; $\theta_Z = 270°$, west.

The relationship between the the body posture with angles (θ_X, θ_Y) and body orientation with θ_Z, based on a belt-worn horizontal phone, is described in Table I.

Table I shows that angles (θx, θy) can be used to recognize the upright and tilted postures. For example, when the posture is stand or sit upright (Sit-U), the X-axis is vertical, then $\theta x \asymp 0°$ and $\theta y \asymp \pm 90°$; otherwise, when the body posture is sit-tilted forward (Sit-F), back (Sit-B), right (Sit-R), or left (Sit-L), then $|\theta_X| > 0°$, or $|\theta_Y| < 90°$, in theory. The values need to be calibrated in the practice, as shown in Fig. 5. Hence, it is possible to classify the lying, tilted and upright postures by combining the acceleration and orientation angles.

TABLE II
EXPERIMENTAL RESULTS FOR INDOOR USING THE MULFUSION ALGORITHM

True:	f-lyi.	f-sitT	p-fall	n-lyi.	bend	sit	stand	sitT	sitS
f-lyi.	122			12	25	2			
f-sitT		119							
p-fall			9						
n-lyi.	4	2		72					
bend					69				
sit		6	1			128	23		
stand		1			7	20	137		
sitT								18	
sitS									18
total	126	126	12	84	101	150	160	18	18
Acc.%	96.8	94.4	75	85.7	68.3	85.3	85.6	100	100
Cohen's Kappa					83.8%				

Fig. 5. Dataset (θ_X, θ_Y) measured from different tilted postures. If $|\theta_X| > (0° + \theta_{\mathrm{Cali}X})$ or $|\theta_Y| < (90° - \theta_{\mathrm{Cali}Y})$, then the posture must be tilted. Here $\theta_{\mathrm{Cali}X}$ or $\theta_{\mathrm{Cali}Y}$ is the empirical calibration value.

C. Fine-Grained Indoor and Outdoor Localization

For the indoor localization, a predeployed RFID network was used to identify the users' ID and their position [31], [32]. The tracking environment (E) was divided into several subareas based on the user's daily activities. The R_{SS} sensed by the reader network and the subarea structure of the environment are symbolized as

$$R_{SS} = \bigcup_{r=1}^{q} R_{SSr} \;;\; E = \bigcup_{j=1}^{m} L_j \quad \begin{cases} q = 1, 2, 3, \dots \\ m = 1, 2, 3, \dots \end{cases} \quad (2)$$

where R_{SS_r} R_{SSr} is the RF signal strength sensed by each of the readers $R_1, R_2, \dots, R_q$, q is the number of readers, L_j denotes the location name of each of the subareas in the environment E, such as $E(L_1, L_2, \dots, L_m) = \{\text{bed1}, \text{sofa}, \text{dining}, \dots\}$, and m is the number of subareas.

The collected training set from each of the subareas is organized as follows:

$$(R_{SS}(i), L(i)) = (R_{SS1}(i), R_{SS2}(i), \dots, R_{SSq}(i), L(i))$$
$$\{i = 1, 2, \dots, n \ \& \ L(i) \in E(L_1, L_2, \dots, L_m)\} \quad (3)$$

where n is the total number of samples in the training set, $Rss(i)R_{SS}(i)$ is the set of signal strengths sensed by several *readers* at the ith ith training point, $L(i)$ is a manually labeled location name of the subareas for the ith ith training point, where $L(i) \in E(L_1, L_2, \dots, L_m)$, and m is the total number of subareas.

A function $f(R_{ss}, E)$ for the relationship between the R_{SS} and each of the subareas in the tracking environment E is learned by a support vector machine (SVM) classifier with a radial basis function (RBF)

Fig. 6. Fine-grained radio map for outdoor (left) and indoor (right) environments.

from the training set as shown in the following equation:

$$f(R_{SS}, E) = \sum_{i=1}^{n} \omega_i k(R_{SS}(i), L(i)) \quad (4)$$

where ω_i is a set of weighted parameters, k is a function relating to the relationship between $R_{SS}(i)$ and $L(i)$ $Rss(i)$ and $L(i)$. Both weights ω_i and function k need to be automatically learned using the SVM classifier. A software package LibSVM [33], which supports multiclass classification, was used to implement the algorithms. The SVM classifier has very good classification ability for previously unseen data [34]. The RBF kernel has less parameters than other nonlinear kernels. Further details about an optimal SVM model selection have been introduced in [34].

After the training model function $f(R_{ss}, E)$ has been obtained during the offline learning phase, the trained model can be used, in an online fashion, to classify the location of a tagged subject. In this phase, the sensed R_{SS} union at each time t will be an input value of the function. The output for each time t will be a subarea name automatically translated by the training model function as shown in the following equation:

$$(t, \text{tag}_{\mathrm{ID}}, R_{SS1}(t), R_{SS2}(t), \dots, R_{SSq}(t)) \stackrel{f(R_{SS}, E)}{\rightarrow}$$
$$(t, \text{tag}_{\mathrm{ID}}, L(t)) \quad (5)$$

where $R_{SS}(t)$ $Rss(t)$ is the RF signal strength sensed by the reader network at time t, tag_{ID} is the tag identity number and also stands for the tagged person, and $L(t)$ is a corresponding subarea name to the input at time t.

For outdoor localization, GPS embedded in the smartphone was used as the outdoor location provider. A fine-grained radio map for a given subarea-structured environment can be created using radio fingerprinting, based on data acquired from GPS [35]. This map generates probability distribution geocoordinate values of GPS (t, latitude, longitude) for a predefined subarea name. Live GPS values are compared to the fingerprint to find the closest match and generate a predicted subarea.

In the initial stage, the outdoor enviroment included six areas (home, garden, park, campus, shop, and hospital) as shown in Fig. 6(left). For the indoor environment, each of the six rooms was divided into two or three functional subareas as shown in Fig. 6(right). For efficiency, we did not get the location name from a GPS map, since it slowed the system speed. Hence, one subject walked around these six areas and recorded the dataset (latitude, longitude, position) as the training set to obtain the initial small fine-grained model for outdoor localization.

C. Falls Detection

The identification of motion and motionless postures classification has been presented in our previous work [34], [36], [37]. In this paper, we focus at a higher algorithmic level, on how to recognize falls based

on fused heterogeneous contexts (current posture, posture transition, position, heart rate), to improve the reliability and accuracy of fall detection. All data were saved in an SQLite Database within the phone that comprises four tables named as: posture, location, minutData, and fusion, respectively.

The posture table was derived from the posture classification based on the dataset $(t, Ax, Ay, Az, \theta_X, \theta_Y, \theta_Z)$ sensed from the phone. The sampling frequency from the phone was set at 5 Hz, and postures classification was performed point by point, but the classification results $(t, posture)$ were saved into the posture table every 2 s using a majority voting mechanism for every classified period of time [33].

The location table is derived from the location classification based on the dataset $(t, tag_{ID}, R_{SS1}, R_{SS2}, R_{SS3})$ sensed from the RFID network (sampling rate for three readers is 2.5 Hz in this study), the location detection results $(t, tag_{ID}, location)$ were saved into the location table every 30 s.

The minutData table was derived from the smartwatch based on the HiCling software development kit, which included $(t, heartrate, isWear)$. The dataset was saved into minutData every minute.

The fusion table was derived from the above three tables. Items $(t, tag_{ID}, currPosture, prePosture, location, heartrate)$ were selected and inserted into the fusion table every 2 s. Since the three tables have different sampling frequency as described previously (2 s versus 30 s versus 60 s), the items will repeat the previous value if a new sample value has not been acquired.

The falls detection is performed based on the fusion table, comprising the heterogeneous, multimodal data. So for example, if a lying or sit-tilted posture was detected, then a *backward reasoning algorithm* was used to check the saved previous posture, current position, and heart rate to infer whether a certain fall or a possible fall can be inferred based on two models: certain fall model and possible fall model, defined next.

$$\text{certainFall} \equiv \text{IsCurrentPosture} (\exists \text{lying}||\text{sitTilt, yes})$$
$$\wedge \text{IsPrePosture} (\exists \text{walk} ||\text{run}|| \text{stand, yes}) \wedge$$
$$\{\text{IsLocatedIn} (\nexists \text{bed}||\text{sofa, yes}) \vee$$
$$\text{IsHeatrate} (\exists \text{higher}||\text{lower, yes})\}$$
$$\rightarrow \text{fall alert to a caregiver immediately}$$

$$\text{possibleFall} \equiv \text{IsCurrentPosture} (\exists \text{lying}||\text{sitTilt, yes})$$
$$\wedge \text{IsPrePosture} (\exists \text{sit, yes}) \wedge$$
$$\{\text{IsLocatedIn} (\nexists \text{bed}||\text{sofa, yes}) \vee$$
$$\text{IsHeatrate} (\exists \text{higher}||\text{lower, yes})\}$$
$$\rightarrow \text{possible alert music with stop button}$$

where the higher or lower heart rate means the measured current heart rate is more than the user's maximum resting heart rate (RHR), or less than the user's minimum RHR, which was tested and saved when the user first began wearing the smartwatch. Zhang *et al.* [38] reported that a healthy RHR for adults is 60–80 bpm and an average adult RHR range is 60–100 bpm. An elevated RHR can be an indicator of increased risk of cardiovascular disease.Certain falls model: Lying or sit tilted from a wrong posture transition (such as from run to lying directly) while located in an inappropriate place (i.e., not the bed or sofa), or sudden change in heart rate.Possible falls model: Lying or sit tilted from a right posture transition (such as from sit to lying), however, located in an inappropriate place (i.e., not the bed or sofa), or sudden change in heart rate. The procedure of the proposed fall detection algorithm (named mulFusion) is shown in Fig. 7. The models demonstrate that the difference between a certain fall (wrong posture transition) and possible fall (right posture transition) is determined by the posture transition. Meanwhile, both models have similar features, e.g., lying or sit tilted at an inappropriate location, or abnormal vital signs, e.g., higher/lower heart rate. If a certain fall is detected, then a fall alert can be delivered to
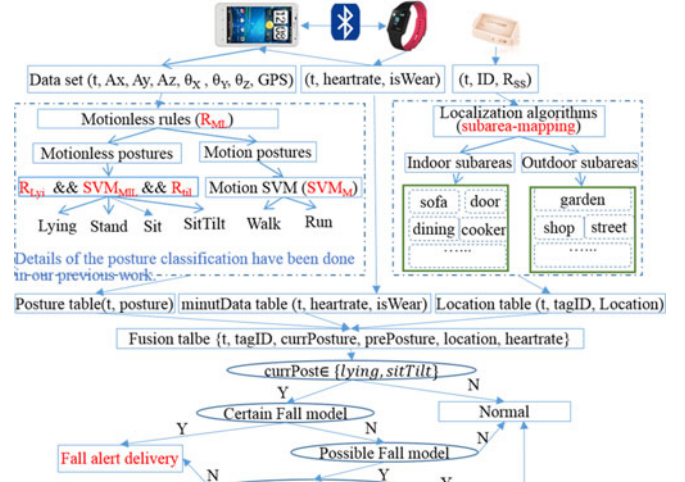

Fig. 7. Fall detection algorithm (mulFusion) based on fused multiple dataset and a certain fall model as well as a possible fall model.

caregivers immediately. Otherwise, alert music with a stop button will play if a possible fall is detected; finally, a fall or a normal lying/sit-tilted activity will be determined according to whether the user stops the alert music.

IV. EXPERIMENTS

In order to evaluate the different situation-awareness outcomes, nine healthy people (four female and five male, aged 25–55) simulated various falls and a set of different daily activities at indoor and outdoor locations. For safety purposes, three mats were distributed on the ground in three different rooms. The experimental results were validated against observation notes recorded by two independent observers.

The experimental results for falls detection were compared with an accelerometer with a predefined threshold method described in our previous work [39]. The algorithms were named as mulFusion and accThresh:

mulFusion: Falls were detected based on the multiple fusion contexts including current posture, posture transition, location, and heart rate, as proposed in this paper.

accThresh: Only using the acceleration change with predefined threshold to detect falls, as described in [39].

A. Indoor Experiments

In the indoor environment, each of the nine subjects performed a series of normal and abnormal activities, described ahead, in a random order for three times, and five of the subjects performed the same activities in prescribed order for another three times, respectively. Additionally, three of the subjects then performed the possible falls using approach1 for three times, and using approach2 once, respectively.

1) Fall-lying (**f-lyi**): From walk to lying quickly or slowly on the bed, sofa, and ground (mat), respectively.
2) Fall-sitTilted (**f-sitT**): From walk to sit-tilted quickly or slowly on the bed, sofa, and ground (mat), respectively.
3) Possible falls (**p-fall**) approach1: From walk to sit on the ground (mat) for more than 2 s, then lying on the ground (mat).
4) Possible falls (**p-fall**) approach2: In order to simulate the elderly falls that may cause the higher heart rate in a case, required run
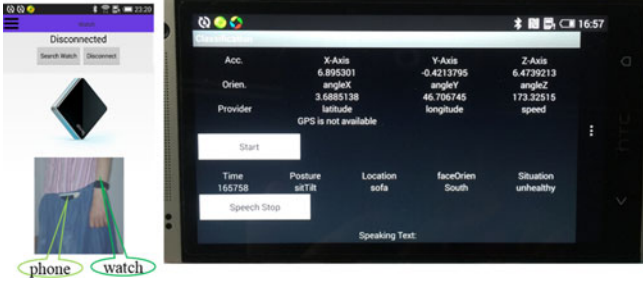
Fig. 8. Interface of the situation-aware system on the phone. Top of the left figure is the phone connecting the watch when using it firstime; bottom of the left figure is a subject wearing the phone and watch at the same time. The right-hand side illustrates the user interface.

TABLE III
COMPARISON OF EXPERIMENTAL RESULTS FOR THREE TYPES OF FALLS WITH NORMAL LYING CLASSIFICATION, USING THE MULFUSION AND ACCTHRESH ALGORITHMS, RESPECTIVELY

	mulFusion algorithm					*accThresh* algorithm				
	f-lyi.	f-sitT	p-fall	n-lyi.	total	f-lyi.	f-sitT	p-fall	n-lyi.	total
TP	122	119	9		250	126	0	9		135
FN	4	7	3		14	0	126	3		129
TN				72	72				0	0
FP				12	12				84	84
total	126	126	12	84	348	126	126	12	84	348
Positive predictive			95.4%					61.6%		
Negative predictive			83.7%					0%		
Sensitivity			94.7%					51.1%		
Specificity			85.7%					0%		

on a treadmill for 15 min first, get the heart rate is more than 90 bpm, then sit tilted on the sofa for a while.

5) Normal lying (**n-lyi**) approach1: From walk to sit on the bed for more than 2 s and then lying on the bed normally.

6) Normal lying (**n-lyi**) approach2: From walk to sit on the bed for less than 2 s, and then lying on the bed very quickly.

7) **Bend**: Do some bending ($>30°$) activity during the walking.

8) Sit tilted (**sitT**): Sit tilted right/left at the sofa for 6 min.

9) Sit still (**sitS**): Sit on a chair and watch television for 65 min.

Following these experiments, there were 126 f-lyi and 126 f-sitT in total (42 on the ground, 42 on the bed, 42 on the sofa); 12 p-fall in total (nine lying on the ground and three sit tilted on the sofa with higher heart rate); 42 normal lying using approach1; 42 normal lying using approach2; 101 Bend, 18 sitT, 18 sitS and a number of standing, walking, as well as sitting activities recorded and analyzed, indoors.

B. Outdoor Experiments

In the outdoor environment, each of the nine subjects walked from home to a park and then adopted the following postures: sit upright or sit back on the park bench for a period of time, and then walk around and bend two times during the walk; finally, sit on the bench again for a while. Thus, there were 18 normal sitting postures and 18 bend postures as well as a number of walking and stand activities recorded.

The outdoors localization was based on the coarse-grained subareas, for instance, GPS location may recognize the park area correctly, but it cannot recognize the bench area within the park. In this case, a possible fall can be raised if the user is sit tilted at the park (bench), since the system deems that the user is sit tilted on the *ground* outdoors.

C. Experimental Results

The postures data collected from the nine subjects were classified in real time and a voice reminder was delivered in real time. The interface of the system is shown in Fig. 8.

The experimental results based on the mulFusion algorithm are shown in Table II.

Table II demonstrates that the level of agreement is very good using the proposed mulFusion algorithm, since its Cohen's Kappa is 83.8%. For example, the accuracy of f-lyi and f-sitT detection were higher (96.8% and 94.4%, respectively). Some instances of f-lyi were classified as normal-lying when the user transitioned from walk to lying on the bed slowly, since in this case, the posture transition was recognized as from standing to lying, rather than from walk to lying.

The accuracy of possible falls (p-fall) classification was 75%. One of the 12 p-fall was classified as sit, since the ending "sit tilted" posture was recognized as sit. Another two of the 12 p-fall were classified as

normal lying, since the lying location ground was misclassified as bed (one of the three mats was located near to the bed). The accuracy of normal-lying (n-lyi) classification was 85.7%. Instances of of normal-lying were classified as f-lyi when the sitting period of time was less than 2 s before the normal lying, since in this case, the sitting posture was ignored, thus the posture transition was analyzed as from walk to lying directly. The accuracy of bend classification was lower (68.3%). Since the "deep waist bend" (more than 70°) has similar features (acceleration and phone's orientation angles) with lying when the phone was belt-worn on the waist, therefore, instances of bend were classified as f-lyi. In fact, bend classification accuracy is problematic, since it depends on dexterity and how much deep bending the users have done.

The classification accuracy for normal sit and stand were similar around 85%. Sit and stand were confused on occassion. The classification accuracy for unhealthy postures sit tilted (sitT) for more than 5 min and sit-still (sitS) for more than one hour all were 100%. For comparison, three types of falls with normal lying activity were classified using the mulThresh algorithm and accThresh algorithm, respectively. The experimental results (see Table III) were compared between both algorithms from four aspects: recognize real falls correctly (TP); recognize real falls as nonfall (FN); recognize nonfall activities correctly (TN); recognize nonfalls as a fall (FP).

Table III illustrates that the algorithm mulFusion can improve the falls detection accuracy and reliability significantly compared to the algorithm accThresh. The classification results for the three types of falls with normal lying, compared to accThresh, mulFusion had positive predictive value of 95.4% versus 61.6%, negative predictive value of 83.7% versus 0%, sensitivity of 94.7% versus 51.1%, and specificity of 85.7% versus 0%. The accThresh algorithm was able to detect all the falls ending with lying (f-lyi) correctly, nevertheless, it recognized 0/126 falls ending with sit tilted (f-sitT) and 0/84 of normal lying (n-lyi), since the normal lying posture also caused a large acceleration changing. For the 12 p-fall, it also only recognized the 9/12 correctly, which was ending with lying. Therefore, this threshold only algorithm was limited for the falls ending with sit-tilted situations.

In general the participants deemed the system helpful and easy to use. It is appareent that the "possible" fall music with a stop button can reduce the delivery of incorrect alerts.

V. CONCLUSION AND FUTURE WORK

The accuracy of falls detection algorithms reported in the literature is good. However, most of the accelerometer-based experiments involved typical falls with a high acceleration upon the impact with the ground.

Slow falls and normal lying are more difficult to detect. Fall-like events, which trigger false alarms, limit users' acceptance. The contribution of this paper is the development of a real-time situation-aware system for falls alert and unhealthy postures reminder, based on integrated multiple contexts (e.g., postures, transition, location, and heart rate) acquired from sensors embedded in a smartphone, in a smartwatch and using a deployed RFID network in an indoor environment.

Fall detection algorithms based on integrated multiple contexts can improve the accuracy of detection of certain falls distinguishing them from normal daily activities. Gjoreski *et al.* [17] studied a combination of body-worn inertial and location sensors for fall detection. They illustrated that the two types of sensors combined with context-based reasoning can significantly improve the performance. Compared to their study, this research combined four modalities (accelerometers, orientation, location, and heart rate). It is potentially more robust. This context-based work can be extended beyond determining falls. The postures sit tilted and sit still may, under certain circumstances, be defined as unhealthy postures. We know that back pain, neck pain, or shoulder pain can be avoided or managed by correcting posture; however, it can be difficult to maintain appropriate postures throughout the day. One of the most common causes of low back pain is poor sitting posture (e.g., sit tilted for a long time) [40]. Hence, it may be possible using this approach to remind people to correct poor postures in real time.

The accuracy of falls detection depends on the accuracy of posture classification and location detection. There are many sources of potential interference in a real living environment, such as electrical and magnetic interference (from electricity and fluorescent devices and even home-based networks). These are much harder to control than in a laboratory situation. In addition, there will be errors introduced by artefact, and absence of GPS signal outdoors. Such issues can be addressed in a longer study, once the technical feasibility, usability, and potential acceptance issues have been overcome or at least better understood. Services could be implemented in two ways: 1) alert can be delivered to caregivers immediately if a certain fall is detected; 2) music with a stop button can play if a possible fall is raised. A fall or a normal lying activity will be determined according to whether the user stops the alert music.

A study by van Hees *et al.* [41] has suggested that the classifier performance can be overestimated using controlled datasets. In future, we will study how to improve classification accuracy for an array of postures and transitions, and inferred situations in real-life conditions, especially for elderly at their home environments. In addition, smartphone-based solutions may have usability issues, since it is a requirement for the user to keep a smartphone at the fixed position [12]. As sensing technology continues to evolve, the use of a smartwatch for an additional channel of accelerometer data is worthy of further investigation. The phone can then be used for data analysis and reminders delivery, which may improve acceptance. The use of such technology for influencing longer term behavior change using real-time reminders requires further study of a longer period.

ACKNOWLEDGMENT

REFERENCES

[1] C. D. Nugent, M. D. Mulvenna, X. Hong, and S. Devlin, "Experiences in the development of a smart lab," *Int. J. Biomed. Eng. Technol.*, vol. 2, no. 4, pp. 319–331, 2009.

[2] J. Teno, D. P. Kiel, and V. Mor, "Multiple stumbles: A risk factor for falls in community-dwelling elderly," *J. Amer. Geriatrics Soc.*, vol. 38, no. 12, pp. 1321–1325, 1990.

[3] B. Najafi, K. Aminian, F. Loew, Y. Blanc, and P. A. Robert, "Measurement of stand-sit and sit-stand transitions using a miniature gyroscope and its application in fall risk evaluation in the elderly," *IEEE Trans. Biomed. Eng.*, vol. 49, no. 8, pp. 843–851, Aug. 2002.

[4] M. B. King and M. E. Tinetti, "Falls in community-dwelling older persons," *J. Amer. Geriatrics Soc.*, vol. 43, no. 10, pp. 1146–1154, 1995.

[5] G. Demiris and B. K. Hensel, "Technologies for an aging society: A systematic review of "smart home" applications," *Yearbook Med. Informat.*, vol. 3, pp. 33–40, 2008.

[6] H. Hawley-Hague and E. Boulton, "Older adults' perceptions of technologies aimed at falls prevention, detection or monitoring: A systematic review," *Int. J. Med. Informat.*, vol. 83, no. 6, pp. 416–426, 2014.

[7] A. Staranowicz, G. R. Brown, and G.-L. Mariottini, "Evaluating the accuracy of a mobile Kinect-based gait-monitoring system for fall prediction," presented at the 6th Int. Conf. Pervasive Technol. Related Assistive Environ., New York, NY, USA, 2013, Paper 57.

[8] U. Anliker *et al.*, "AMON: A wearable multiparameter medical monitoring and alert system," *IEEE Trans. Inf. Technol. Biomed.*, vol. 8, no. 4, pp. 415–427, Dec. 2004.

[9] *Fall* Detector *MCT-241MD PERS*, Visonic Inc., Tel Aviv, Israel, 2016. [Online]. Available: http://www.visonic.com/Products/Wireless-Emergency-Response-Systems/Fall-detector-mct-241md-pers-wer

[10] M. Kangas, A. Konttila, I. Winblad, and T. Jamsa, "Determination of simple thresholds for accelerometry-based parameters for fall detection," in *Proc. 29th Annu. Int. Conf. IEEE Eng. Med. Biol. Soc.*, 2007, pp. 1367–1370.

[11] U. Lindemann, A. Hock, M. Stuber, W. Keck, and C. Becker, "Evaluation of a fall detector based on accelerometers: A pilot study," *Med. Biol. Eng. Comput.*, vol. 43, no. 5, pp. 548–551, 2005.

[12] S. Abbate, M. Avvenuti, F. Bonatesta, and G. Cola, "A smartphone-based fall detection system," *Pervasive Mobile Comput.*, vol. 8, no. 6, pp. 883–899, 2012.

[13] J. T. Zhang, A. C. Novak, B. Brouwer, and Q. Li, "Concurrent validation of XSENS MVN measurement of lower limb joint angular kinematics," *Physiol. Meas.*, vol. 34, no. 8, pp. N63–N69, 2013.

[14] F. Bianchi, S. J. Redmond, M. R. Narayanan, S. Cerutti, and N. H. Lovell, "Barometric pressure and triaxial accelerometry-based falls event detection," *IEEE Trans. Neural Syst. Rehabil. Eng.*, vol. 18, no. 6, pp. 619–627, Dec. 2010.

[15] Q. Li, J. A. Stankovic, M. A. Hanson, A. T. Barth, J. Lach, and G. Zhou, "Accurate, fast fall detection using gyroscopes and accelerometer-derived posture information," in *Proc. 6th Int. Workshop Wearable Implantable Body Sensor Netw.*, Jun. 2009, pp. 138–143.

[16] M. Lustrek and B. Kaluza, "Fall detection and activity recognition with machine learning," *Informatica*, vol. 33, no. 2, pp. 197–204, 2009.

[17] H. Gjoreski, M. Gams, and M. Luštrek, "Context-based fall detection and activity recognition using inertial and location sensors," *J. Ambient Intell. Smart Environ.*, vol. 6, no. 4, pp. 419–433, 2014.

[18] N. Y. Ko and T. Y. Kuc, "Fusing range measurements from ultrasonic beacons and a laser range finder for localization of a mobile robot," *Sensors*, vol. 15, no. 5, pp. 11050–11075, 2015.

[19] T. Yamazaki, "Beyond the smart home," in *Proc. Int. Conf. Hybrid Inf. Technol.*, 2006, pp. 350–355.

[20] C. C. Hsu and P. C. Yuan, "The design and implementation of an intelligent deployment system for RFID readers," *Expert Syst. Appl.*, vol. 38, no. 8, pp. 10506–10517, 2011.

[21] J.-H. Seok, J.-Y. Lee, C. Oh, J.-J. Lee, and H. J. Lee, "RFID sensor deployment using differential evolution for indoor mobile robot localization," in *Proc. IEEE Int. Conf. Intell. Robots Syst.*, 2010, pp. 3719–3724.

[22] A. T. Murray, K. Kim, J. W. Davis, R. Machiraju, and R. E Parent, "Coverage optimization to support security monitoring," *Comput., Environ. Urban Syst.*, vol. 31, no. 2, pp. 133–147, 2007.

[23] F. Y. S. Lin and P. L. Chiu, "A simulated annealing algorithm for energy efficient sensor network design," in *Proc. 3rd Int. Symp. Model. Optim. Mobile, Ad Hoc, Wireless Netw.*, 2005, pp. 183–189.

[24] A. W. Reza and T. K. Geok, "Investigation of indoor location sensing via RFID reader network utilizing grid covering algorithm," *J. Wireless Pers. Commun.*, vol. 49, no. 1, pp. 67–80, 2009.

[25] J. Hightower, R. Want, and G. Borriello, "SpotON: An indoor 3D location sensing technology based on RF signal strength," Univ. Washington, Seattle, WA, USA, Tech. Rep. UW CSE 00-02-02, 2000.

[26] J. Zhou and J. Shi, "RFID localization algorithms and applications—A review," *J. Intell. Manuf.*, vol. 20, no. 6, pp. 695–707, 2009.

[27] K. Lorincz and M. Welsh, "MoteTrack: A robust, decentralized approach to RF-based location tracking," *Pers. Ubiquitous Comput.*, vol. 11, no. 6, pp. 489–503, 2007.

[28] X. Nguyen, M. I. Jordan, and B. Sinopoli, "A kernel-based learning approach to ad hoc sensor network localization," *ACM Trans. Sensor Netw.*, vol. 1, no. 1, pp. 134–152, 2005.

[29] L. M. Ni, Y. Liu, Y. C. Lau, and A. P. Patil, "LANDMARC: Indoor location sensing using active RFID," *Wireless Netw.*, vol. 10, no. 6, pp. 701–710, 2004.

[30] S. Zhang, P. McCullagh, J. Zhang, and T. Yu, "A smartphone based real-time daily activity monitoring system," *Cluster Comput.*, vol. 17, no. 3, pp. 711–721, 2014.

[31] S. Zhang, P. McCullagh, C. Nugent, H. Zheng, and N. Black, "A subarea mapping approach for indoor localisation," in *Toward Useful Services for Elderly and People With Disabilities*. Berlin, Germany: Springer-Verlag, 2011, pp. 80–87.

[32] S. Zhang, P. McCullagh, H. Zhou, Z. Wen, and Z. Xu, "RFID network deployment approaches for indoor localisation," in *Proc. 12th Int. Conf. Wearable Implantable Body Sensor Netw.*, Boston, MA, USA, 2015, pp. 1–6.

[33] C.-C. Chang and C.-J. Lin, "LIBSVM: A library for support vector machines," *ACM Trans. Intell. Syst. Technol.* vol. 2, no. 3, 2011, Art. no. 27. [Online]. Available: http://www.csie.ntuedu.tw/cjlin/libsvm

[34] S. Zhang, P. McCullagh, C. Nugent, H. Zheng, and M. Baumgarten, "Optimal model selection for posture recognition in home-based healthcare," *Int. J. Mach. Learn. Cybern.*, vol. 2, no. 1, pp. 1–14, 2011.

[35] Y. Kim, Y. Chon, and H. Cha, "Smartphone-based collaborative and autonomous radio fingerprinting," *IEEE Trans. Syst., Man, Cybern. C*, vol. 42, no. 1, pp. 112–122, Jan. 2012.

[36] S. Zhang, P. Mccullagh, C. Nugent, and H. Zheng, "Activity monitoring using a smart phone's accelerometer with hierarchical classification," in *Proc. 6th Int. Conf. Intell. Environ.*, 2010, pp. 158–163.

[37] S. Zhang, H. Li, P. McCullagh, C. Nugent, and H. Zheng, "A real-time falls detection system for elderly," in *Proc. 5th Comput. Sci. Electron. Eng. Conf.*, 2013, pp. 51–56.

[38] D. Zhang, X. Shen, and X. Qi, "Resting heart rate and all-cause and cardiovascular mortality in the general population: A meta-analysis," *Can. Med. Assoc. J.*, vol. 188, no. 3, pp. E53–E63, 2016.

[39] S. Zhang, P. McCullagh, C. Nugent, and H. Zheng, "A theoretic algorithm for fall and motionless detection," in *Proc. 3rd Int. Conf. Pervasive Comput. Technol. Healthcare*, 2009, pp. 1–6.

[40] P. J. Mork and R. H. Westgaard, "Back posture and low back muscle activity in female computer workers: A field study," *Clin. Biomech.*, vol. 24, no. 2, pp. 169–175, 2009.

[41] V. T. van Hees, R. Golubic, U. Ekelund, and S. Brage, "Impact of study design on development and evaluation of an activity-type classifier," *J. Appl. Physiol.*, vol. 114, no. 8, pp. 1042–1051, 2013.

Technical Correspondence

Situation Awareness Inferred From Posture Transition and Location: Derived From Smartphone and Smart home Sensors

Shumei Zhang, Paul McCullagh, Huiru Zheng, and Chris Nugent

Abstract—Situation awareness may be inferred from user context such as body posture transition and location data. Smartphones and smart homes incorporate sensors that can record this information without significant inconvenience to the user. Algorithms were developed to classify activity postures to infer current situations; and to measure user's physical location, in order to provide context that assists such interpretation. Location was detected using a subarea-mapping algorithm; activity classification was performed using a hierarchical algorithm with backward reasoning; and falls were detected using fused multiple contexts (current posture, posture transition, location, and heart rate) based on two models: "certain fall" and "possible fall." The approaches were evaluated on nine volunteers using a smartphone, which provided accelerometer and orientation data, and a radio frequency identification network deployed at an indoor environment. Experimental results illustrated falls detection sensitivity of 94.7% and specificity of 85.7%. By providing appropriate context the robustness of situation recognition algorithms can be enhanced.

Index Terms—Assisted living, body sensor networks (BSNs), context awareness, wearable computers.

I. INTRODUCTION

Many studies have utilized intelligent environments to assist elderly or vulnerable people to live independently at home and to potentially maintain their quality of life. One goal of smart homes is to monitor lifestyle (such as activities and locations) of the occupant in order to promote autonomy and independent living and to increase feelings of security and safety. Sensing technology of various forms has been employed to track the activities and locations within the home environment. Derived information can be used as input to control domestic devices such as lighting, heater, television, and cooker based on a user's current activity and location [1]. Radio frequency (RF) identification (RFID), body sensor networks (BSNs), and wireless sensor networks (WSNs) are complementary technologies used in this research environment. RFID can identify and track the location of tagged occupants, BSNs can record movement, orientation, and biosignals, and WSNs can discover and record attributes within and about the environment

(e.g., temperature, status of doors and windows). All components have the capacity to communicate wirelessly and be connected as an "Internet of Things," providing an associated "big data" resource, usually of unstructured data yielding a potential interpretation and understanding problem for the researcher. If this problem can be successfully addressed, then knowledge regarding identity, activity, location, and environmental conditions can be derived by integrating data from RFID with BSNs and WSNs. This vision drives an area of significant research effort, which may be classified as "situation awareness" leading to situation recognition. The research poses challenges for communications infrastructure, connected health monitoring, and acceptance of technology by the user; much of which relies upon computing advances.

The World Health Organization estimated that 424 000 fatal falls occur each year, making falls a leading cause of accidental deaths. Elderly people over 70 years have the highest risk of fatal falls, more than 32% of older persons have experienced a fall at least once a year with 24% encountering serious injuries [2], [3]. Approximately 3% of people who experience a fall remain on the ground or floor for more than 20 min prior to receiving assistance [4]. A serious fall decreases an older person's self-confidence and motivation for independence and even for remaining in his/her own home. Therefore, a situation awareness system can assist frail people living at home and potentially sustain a good quality of life for longer.

The aim of this work is to combine smartphone and smart home technology to provide context on posture transition and location. This research developed a monitoring system to identify users' activities, locations, and hence to infer users' current situations; should an abnormal situation be classified then an alert may be delivered to the user or to a guardian, if necessary. In particular, we attempt to detect falls and posture transitions using BSNs and an RFID-enabled smart home.

The paper is organized as follows. Related work is discussed in Section II, and methodologies for the system configuration and current situation detection algorithms are described in Section III. The experiments undertaken and results obtained are presented in Section IV. Section V focuses on discussion, limitations of the approach, and future work.

II. RELATED WORK

A. Detection of Falls

Falls may be detected by using devices such as environment-embedded sensors and wearable sensors. Wireless optical cameras can be embedded in a tracking environment [5]; however, they can only monitor fixed places and there can be privacy protection issues to resolve for smart home occupants [6]. Depth-based sensors such as Kinect [7] do not reproduce images and can overcome acceptance issues. Such devices are feasible and maybe useful at high-risk

locations for falls. Wearable sensors comprising gyroscopes, tilt sensors, and accelerometers allow users to be monitored within and outside of their home environment. Such sensors can be integrated into existing community-based alarm and emergency systems [8]. For example, the MCT-241MD PERS [9] is a commercial product that detects falls. A built-in tilt sensor and a manual emergency alert button can trigger a call to a remote monitoring station for help, when tilts of more than 60° lasting more than a minute are detected.

Kangas *et al.* [10] investigated acceleration of falls from sensors attached to the waist, wrist, and head, and demonstrated that measurements from the waist and head were more useful for fall detection. Lindemann *et al.* [11] quantified fall detection using two head-worn accelerometers that offer sensitive impact detection for heavy falls based on three predefined thresholds. Smartphone sensors also face usability and acceptance issues, particularly if required to be worn in a predetermined position (e.g., waist) and orientation [12]. Whilst they may not yet provide a "real living" solution, a system based on a smartphone does not suffer the same obstacles of setup time and stigmatization as dedicated laboratory sensors systems such as XSENS [13]. Hence, it is worthwhile determining whether using a phone can be beneficial for inferring "situations." Their pervasive nature, computational power, connectedness, and multifunction capability are clearly advantageous as the phone can deliver real-time feedback and/or alert messages across the full range of communication platforms (telephone, internet, and social media).

Methods that use only the accelerometer with some empirical threshold can lead to many false positives from other "fall-like" activities such as sitting down quickly and jumping, which feature a large change in vertical acceleration. In order to improve the reliability of fall detection, studies combined accelerometers with other sensors. Bianchi *et al.* [14] integrated an accelerometer with a barometric pressure sensor into a wearable device, and demonstrated that fall detection accuracy improved in comparison to using accelerometer data alone (96.9% versus 85.3%). Li *et al.* [15] combined two accelerometers with gyroscopes on the chest and thigh, respectively, and concluded that fall detection accuracy improved. Machine learning techniques have also been used to improve falls detection and recognition [16], [17].

B. Location Tracking

Location tracking systems are varied in their accuracy, range, and infrastructure costs. The challenges are how to achieve more accurate fine-grained subarea-position estimation while minimizing equipment costs. For localization outdoors, the global positioning system (GPS) works well in most environments. However, the signal from satellites cannot penetrate most buildings, so GPS cannot be used reliably in indoor locations.

Schemes envisioned for indoor localization are mostly based on machine vision, laser range-finding, or cell network localization [18]. The "Ubiquitous Home" [19] was equipped with a variety of sensors, such as cameras, microphones, floor pressure sensors, RFID, and accelerometers to monitor human activities and their location.

There are many challenges associated with RFID deployment in a smart home environment. For example, deployment should consider the facilities arrangement, to deal with missing data caused by interfering, absorbing, or distorting factors, and to ensure best coverage using the minimum number of readers. RFID reader deployment can be assessed by practice in experimental trials or by calculation using mathematical algorithms [20], [21]. The practical approach arranges the readers using
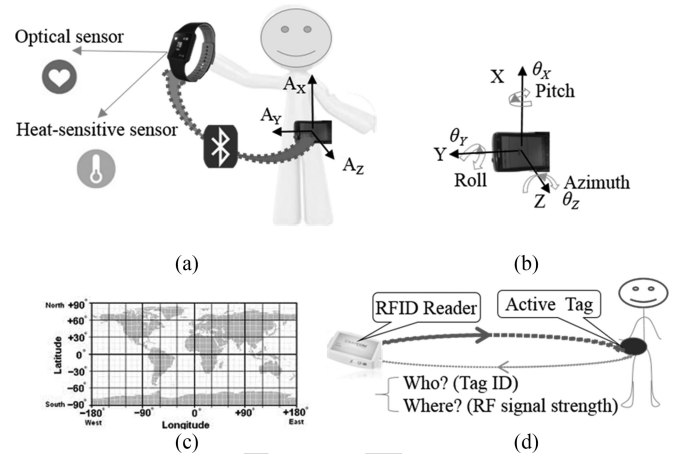

Fig. 1. System configuration; datasets acquired from the phone's sensors, smartwatch's sensors, and RFID networks at indoor: (a) acceleration with heart rate, (b) orientation angles, (c) geocoordinate (latitude, longitude), and (d) RFID networks (ID, R_{SS}).

personal experience [22]. The mathematical approach formulates the sensor deployment as a search algorithm. Algorithms investigated include generic search and simulated annealing [23]. Reza and Geok [24] introduced a geometric grid-covering algorithm for reader deployment inside buildings and achieved an average accuracy of 0.6 m.

RFID localization methods can be classified into two categories: 1) position is estimated by using distances calculated based on a signal propagation model; 2) position is estimated by using RF signal strength (R_{SS}) directly. In 1), the position of a target subject is triangulated in the form of coordinates (distances between the tag and each of the fixed readers), based on an empirical RF propagation model [25], [26]. In 2), the R_{SS} values are mapped onto a defined physical area based on a number of reference nodes using their known positions. Using this method, it is possible to reduce the errors caused by the translation from R_{SS} to distance, as it avoids use of the RF signal propagation model. Learning approaches have been based upon the k-NN algorithm [27], [28] or a kernel-based algorithm [29].

The research discussed in this paper detects falls based on integrated multiple contexts, e.g., activity postures, location, and heart rate.

III. METHODOLOGY

We developed and subsequently evaluated a situation-aware system using a smartphone, which could infer activity from a users' posture, posture transition, and their current position. Detection of falls provides an exemplar but other activities can be inferred.

A. System Configuration

The hardware comprised an HTC802w smartphone connected with a HiCling smartwatch and an RFID network. The system configuration is shown in Fig. 1. The phone connects with the watch via Bluetooth, and communicates with the RFID reader via WiFi. Feedback was delivered via the phone using voice and text messages.

The phone's processor operated at 1.7 GHz, the memory capacity was 2 GB with an additional 32 GB memory card and the operating system was Android 4.4.3. The phone embedded ten types of sensors, but only GPS, 3-axis accelerometer, and the orientation sensors were used.

The phone was belt-worn on the left side of the waist in a horizontal orientation. In this case, the accelerometer coordinate system is that the
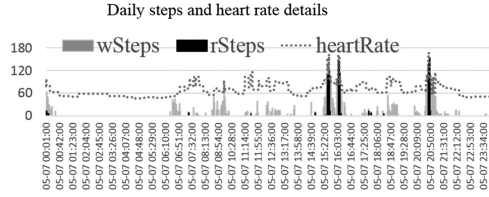
Fig. 2. Heart rate measurement compared to walk and run steps. The heart rate intensity zone can be used for physical activity intensity analysis.
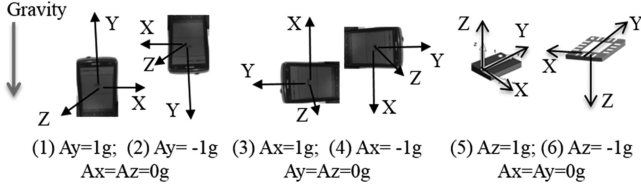

Fig. 3. Six 3-D coordinate systems based on the phone's orientation.

Fig. 4. Relationship between the body postures and maximum value of ($|Ax|$, $|Ay|$, $|Az|$).

TABLE I
BODY POSTURES WITH 3-D ROTATION ANGLES (θx, θy, θz)

Tilted angles (θ_X, θ_Y)		Body postures	Orientation angle θ_Z [0°, 360°]	Orientation
θ_X [−180°, 180°]	θ_Y [−90°, 90°]			
$\leq 0 + \theta_{caliX}$	$\geq 90 - \theta_{caliY}$	Upright	0 or 360	North
$\leq 0 + \theta_{caliX}$	$\leq 90 - \theta_{caliY}$	Tilted right	90	East
$\theta_{caliX} \leq |\theta_X| \leq 90$	$\leq 90 - \theta_{caliY}$	Tilted back	180	South
$\geq 180 - \theta_{caliX}$	$\geq 90 - \theta_{caliY}$	Tilted left	270	West

Here $\theta_{CaliX} = 10$, $\theta_{CaliY} = 20$ are empirical calibration values.

X-axis is vertical, the Y-axis is horizontal, and the Z-axis is orthogonal to the screen, as shown in Fig. 1(a). The phone's orientation can be monitored using the orientation sensor. This sensor provides three-dimensional (3-D) rotation angles along the three axes (*pitch, roll, azimuth*), denoted as (θ_X, θ_Y, θ_Z), as depicted in Fig. 1(b).

Fig. 2 shows a user's daily steps of walk and run as well as instantaneous heart rate, obtained from the smartwatch.

The smartwatch was embedded with optical sensor, 3-D accelerometer, captive skin touch sensor, and Bluetooth 4.0. The minute-based dataset accessed from the watch provides a parameter set (*t, wSteps, rSteps, heartrate, isWear*). The parameter isWear indicates whether the user has watch on, wSteps is walking steps, rSteps is run steps.

The outdoor localization is determined via GPS using the geocoordinate (latitude, longitude) as shown in Fig. 1(c). The indoor localization is recognized via a predeployed RFID network. The position (where?) is determined by received RF signal strength (R_{SS}); identity (who?) is provided by RFID tag ID, as shown in Fig. 1(d). The RFID reader/active tag frequency was 868 MHz, with a theoretical detection range of up to 8 m.

B. Data Acquisition

Five datasets: 3-D acceleration (*t, Ax, Ay, Az*), 3-D orientation angles (*t*, θ_X, θ_Y, θ_Z), vital signs signal (*t, heartrate, isWear*), geocoordinates (*t*, latitude, longitude), and RFID data series of (*t*, ID, R_{SS}) were obtained. Subsequently, the datasets were used for the evaluation of the posture classification, location recognition, and by further processing to infer fall detection.

1) Acceleration: For a tri-axis accelerometer, six 3-D coordinate systems are apparent (vertical axis is *X, Y,* or *Z* in upward or downward directions) according to the phone's orientation, as shown in Fig. 3 (1)–(6).

Fig. 3 illustrates the tri-axis directions determined by the phone's orientation. The absolute value of vertical acceleration is equal to the maximum stationary value among ($|A_x|$, $|A_y|$, $|A_z|$) as shown in the following equation:

$$|A_{\mathrm{vertical}}| = \mathrm{Max}\,(|A_x|, |A_y|, |A_z|). \qquad (1)$$

Equation (1) declares that the vertical-axis acceleration depends on the orientation, so postures (such as lying) can be inferred according to the vertical-axis shifts among (Ax, Ay, Az), as shown in the acceleration patterns in Fig. 4.
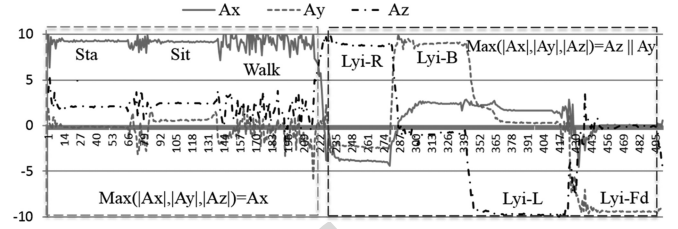
If the upper body posture is upright (stand, sit, or walk), then the maximum absolute acceleration is Ax, and the X-axis is vertical, since the phone has horizontal orientation. If the body posture is lying right, lying back, lying left, or lying face down, then the vertical axis is the Y- or Z-axis, so the maximum value of ($|Ax|$, $|Ay|$, $|Az|$) must be Ay or Az. In theory, one axis may indicate the influence of acceleration due to gravity (± 9.81 m/s^2) and the other two should be zero. In practice, orientation somewhat between states, transition in orientation, movement, and artifact impose relative noise making transitions less precise. Further details on methodology and heuristic classification rules to infer posture by accelerometry are provided in [30].

2) Orientation Angles: The orientation sensor provides 3-D rotation angles along the three axes (pitch, roll, azimuth) are denoted as (θ_X, θ_Y, θ_Z).

1) Pitch (θ_X), degrees of rotation around the X-axis, the range of values is [−180°, 180°], with positive values when the positive Z-axis moves toward the positive Y-axis.
2) Roll (θ_Y), degrees of rotation around the Y-axis, $-90° <= \theta_Y <= 90°$, with positive values when the positive Z-axis moves towards the positive X-axis.
3) Azimuth (θ_Z), degrees of rotation around the Z-axis, $\theta_Z = $ [0°, 360°]. It is used to detect the compass direction. $\theta_Z = 0°$ or 360°, north; $\theta_Z = 180°$, south; $\theta_Z = 90°$, east; $\theta_Z = 270°$, west.

The relationship between the the body posture with angles (θ_X, θ_Y) and body orientation with θ_Z, based on a belt-worn horizontal phone, is described in Table I.

Table I shows that angles (θx, θy) can be used to recognize the upright and tilted postures. For example, when the posture is stand or sit upright (Sit-U), the X-axis is vertical, then $\theta x \asymp 0°$ and $\theta y \asymp \pm 90°$; otherwise, when the body posture is sit-tilted forward (Sit-F), back (Sit-B), right (Sit-R), or left (Sit-L), then $|\theta_X| > 0°$, or $|\theta_Y| < 90°$, in theory. The values need to be calibrated in the practice, as shown in Fig. 5. Hence, it is possible to classify the lying, tilted and upright postures by combining the acceleration and orientation angles.

TABLE II
EXPERIMENTAL RESULTS FOR INDOOR USING THE MULFUSION ALGORITHM

True:	f-lyi.	f-sitT	p-fall	n-lyi.	bend	sit	stand	sitT	sitS
f-lyi.	122			12	25	2			
f-sitT		119							
p-fall			9						
n-lyi.	4		2	72					
bend					69				
sit		6	1			128	23		
stand		1			7	20	137		
sitT								18	
sitS									18
total	126	126	12	84	101	150	160	18	18
Acc.%	96.8	94.4	75	85.7	68.3	85.3	85.6	100	100
Cohen's Kappa						83.8%			

Fig. 5. Dataset (θ_X, θ_Y) measured from different tilted postures. If $|\theta_X| > (0° + \theta_{\mathrm{Cali}X})$ or $|\theta_Y| < (90° - \theta_{\mathrm{Cali}Y})$, then the posture must be tilted. Here $\theta_{\mathrm{Cali}X}$ or $\theta_{\mathrm{Cali}Y}$ is the empirical calibration value.

C. Fine-Grained Indoor and Outdoor Localization

For the indoor localization, a predeployed RFID network was used to identify the users' ID and their position [31], [32]. The tracking environment (E) was divided into several subareas based on the user's daily activities. The R_{SS} sensed by the reader network and the subarea structure of the environment are symbolized as

$$R_{SS} = \bigcup_{r=1}^{q} R_{SSr} \; ; \; E = \bigcup_{j=1}^{m} L_j \quad \begin{cases} q = 1, 2, 3, \dots \\ m = 1, 2, 3, \dots \end{cases} \quad (2)$$

where R_{SSr} is the RF signal strength sensed by each of the readers $R_1, R_2, \dots, R_q$, q is the number of readers, L_j denotes the location name of each of the subareas in the environment E, such as $E(L_1, L_2, \dots, L_m) = \{\mathrm{bed1, sofa, dining}, \dots\}$, and m is the number of subareas.

The collected training set from each of the subareas is organized as follows:

$$(R_{SS}(i), L(i)) = (R_{SS1}(i), R_{SS2}(i), \dots, R_{SSq}(i), L(i))$$
$$\{i = 1, 2, \dots, n \, \& \, L(i) \in E(L_1, L_2, \dots, L_m)\} \quad (3)$$

where n is the total number of samples in the training set, $R_{SS}(i)$ is the set of signal strengths sensed by several *readers* at the *i*th training point, $L(i)$ is a manually labeled location name of the subareas for the *i*th training point, where $L(i) \in E(L_1, L_2, \dots, L_m)$, and m is the total number of subareas.

A function $f(R_{ss}, E)$ for the relationship between the R_{SS} and each of the subareas in the tracking environment E is learned by a support vector machine (SVM) classifier with a radial basis function (RBF)
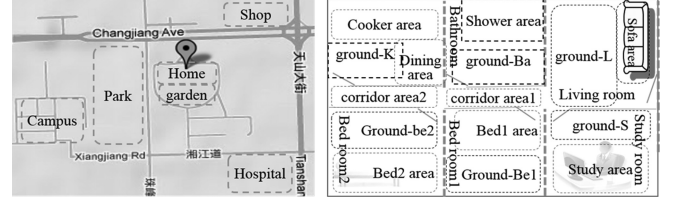

Fig. 6. Fine-grained radio map for outdoor (left) and indoor (right) environments.

from the training set as shown in the following equation:

$$f(R_{SS}, E) = \sum_{i=1}^{n} \omega_i k(R_{SS}(i), L(i)) \quad (4)$$

where ω_i is a set of weighted parameters, k is a function relating to the relationship between $R_{SS}(i)$ and $L(i)$. Both weights ω_i and function k need to be automatically learned using the SVM classifier. A software package LibSVM [33], which supports multiclass classification, was used to implement the algorithms. The SVM classifier has very good classification ability for previously unseen data [34]. The RBF kernel has less parameters than other nonlinear kernels. Further details about an optimal SVM model selection have been introduced in [34].

After the training model function $f(R_{ss}, E)$ has been obtained during the offline learning phase, the trained model can be used, in an online fashion, to classify the location of a tagged subject. In this phase, the sensed R_{SS} union at each time t will be an input value of the function. The output for each time t will be a subarea name automatically translated by the training model function as shown in the following equation:

$$(t, \mathrm{tag_{ID}}, R_{SS1}(t), R_{SS2}(t), \dots, R_{SSq}(t)) \overset{f(R_{SS}, E)}{\rightarrow}$$
$$(t, \mathrm{tag_{ID}}, L(t)) \quad (5)$$

where $R_{SS}(t)$ is the RF signal strength sensed by the reader network at time t, $\mathrm{tag_{ID}}$ is the tag identity number and also stands for the tagged person , and $L(t)$ is a corresponding subarea name to the input at time t.

For outdoor localization, GPS embedded in the smartphone was used as the outdoor location provider. A fine-grained radio map for a given subarea-structured environment can be created using radio fingerprinting, based on data acquired from GPS [35]. This map generates probability distribution geocoordinate values of GPS (t, latitude, longitude) for a predefined subarea name. Live GPS values are compared to the fingerprint to find the closest match and generate a predicted subarea.

In the initial stage, the outdoor enviroment included six areas (home, garden, park, campus, shop, and hospital) as shown in Fig. 6(left). For the indoor environment, each of the six rooms was divided into two or three functional subareas as shown in Fig. 6(right). For efficiency, we did not get the location name from a GPS map, since it slowed the system speed. Hence, one subject walked around these six areas and recorded the dataset (latitude, longitude, position) as the training set to obtain the initial small fine-grained model for outdoor localization.

C. Falls Detection

The identification of motion and motionless postures classification has been presented in our previous work [34], [36], [37]. In this paper, we focus at a higher algorithmic level, on how to recognize falls based

on fused heterogeneous contexts (current posture, posture transition, position, heart rate), to improve the reliability and accuracy of fall detection. All data were saved in an SQLite Database within the phone that comprises four tables named as: posture, location, minutData, and fusion, respectively.

The posture table was derived from the posture classification based on the dataset $(t, Ax, Ay, Az, \theta_X, \theta_Y, \theta_Z)$ sensed from the phone. The sampling frequency from the phone was set at 5 Hz, and postures classification was performed point by point, but the classification results $(t,$ posture$)$ were saved into the posture table every 2 s using a majority voting mechanism for every classified period of time [33].

The location table is derived from the location classification based on the dataset $(t, \text{tag}_{\text{ID}}, R_{SS1}, R_{SS2}, R_{SS3})$ sensed from the RFID network (sampling rate for three readers is 2.5 Hz in this study), the location detection results $(t, \text{tag}_{\text{ID}},$ location$)$ were saved into the location table every 30 s.

The minutData table was derived from the smartwatch based on the HiCling software development kit, which included $(t,$ heartrate, isWear$)$. The dataset was saved into minutData every minute.

The fusion table was derived from the above three tables. Items $(t,$ tag$_{\text{ID}},$ currPosture, prePosture, location, heartrate$)$ were selected and inserted into the fusion table every 2 s. Since the three tables have different sampling frequency as described previously (2 s versus 30 s versus 60 s), the items will repeat the previous value if a new sample value has not been acquired.

The falls detection is performed based on the fusion table, comprising the heterogeneous, multimodal data. So for example, if a lying or sit-tilted posture was detected, then a *backward reasoning algorithm* was used to check the saved previous posture, current position, and heart rate to infer whether a certain fall or a possible fall can be inferred based on two models: certain fall model and possible fall model, defined next.

$$\text{certainFall} \equiv \text{IsCurrentPosture} \,(\exists \text{lying} || \text{sitTilt, yes})$$
$$\wedge \text{IsPrePosture} \,(\exists \text{walk} || \text{run} || \text{stand, yes}) \wedge$$
$$\{\text{IsLocatedIn} \,(\nexists \text{bed} || \text{sofa, yes}) \vee$$
$$\text{IsHeatrate} \,(\exists \text{higher} || \text{lower, yes})\}$$
$$\rightarrow \text{fall alert to a caregiver immediately}$$

$$\text{possibleFall} \equiv \text{IsCurrentPosture} \,(\exists \text{lying} || \text{sitTilt, yes})$$
$$\wedge \text{IsPrePosture} \,(\exists \text{sit, yes}) \wedge$$
$$\{\text{IsLocatedIn} \,(\nexists \text{bed} || \text{sofa, yes}) \vee$$
$$\text{IsHeatrate} \,(\exists \text{higher} || \text{lower, yes})\}$$
$$\rightarrow \text{possible alert music with stop button}$$

where the higher or lower heart rate means the measured current heart rate is more than the user's maximum resting heart rate (RHR), or less than the user's minimum RHR, which was tested and saved when the user first began wearing the smartwatch. Zhang *et al.* [38] reported that a healthy RHR for adults is 60–80 bpm and an average adult RHR range is 60–100 bpm. An elevated RHR can be an indicator of increased risk of cardiovascular disease.Certain falls model: Lying or sit tilted from a wrong posture transition (such as from run to lying directly) while located in an inappropriate place (i.e., not the bed or sofa), or sudden change in heart rate.Possible falls model: Lying or sit tilted from a right posture transition (such as from sit to lying), however, located in an inappropriate place (i.e., not the bed or sofa), or sudden change in heart rate. The procedure of the proposed fall detection algorithm (named mulFusion) is shown in Fig. 7. The models demonstrate that the difference between a certain fall (wrong posture transition) and possible fall (right posture transition) is determined by the posture transition. Meanwhile, both models have similar features, e.g., lying or sit tilted at an inappropriate location, or abnormal vital signs, e.g., higher/lower heart rate. If a certain fall is detected, then a fall alert can be delivered to
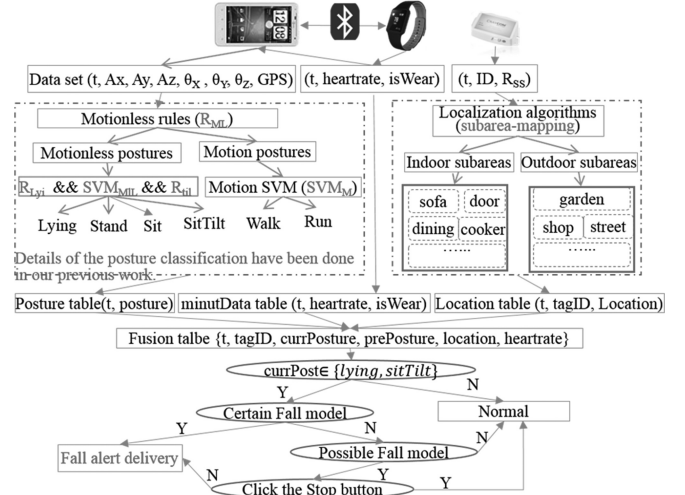

Fig. 7. Fall detection algorithm (mulFusion) based on fused multiple dataset and a certain fall model as well as a possible fall model.

caregivers immediately. Otherwise, alert music with a stop button will play if a possible fall is detected; finally, a fall or a normal lying/sit-tilted activity will be determined according to whether the user stops the alert music.

IV. EXPERIMENTS

In order to evaluate the different situation-awareness outcomes, nine healthy people (four female and five male, aged 25–55) simulated various falls and a set of different daily activities at indoor and outdoor locations. For safety purposes, three mats were distributed on the ground in three different rooms. The experimental results were validated against observation notes recorded by two independent observers.

The experimental results for falls detection were compared with an accelerometer with a predefined threshold method described in our previous work [39]. The algorithms were named as mulFusion and accThresh:

mulFusion: Falls were detected based on the multiple fusion contexts including current posture, posture transition, location, and heart rate, as proposed in this paper.

accThresh: Only using the acceleration change with predefined threshold to detect falls, as described in [39].

A. Indoor Experiments

In the indoor environment, each of the nine subjects performed a series of normal and abnormal activities, described ahead, in a random order for three times, and five of the subjects performed the same activities in prescribed order for another three times, respectively. Additionally, three of the subjects then performed the possible falls using approach1 for three times, and using approach2 once, respectively.

1) Fall-lying (**f-lyi**): From walk to lying quickly or slowly on the bed, sofa, and ground (mat), respectively.
2) Fall-sitTilted (**f-sitT**): From walk to sit-tilted quickly or slowly on the bed, sofa, and ground (mat), respectively.
3) Possible falls (**p-fall**) approach1: From walk to sit on the ground (mat) for more than 2 s, then lying on the ground (mat).
4) Possible falls (**p-fall**) approach2: In order to simulate the elderly falls that may cause the higher heart rate in a case, required run
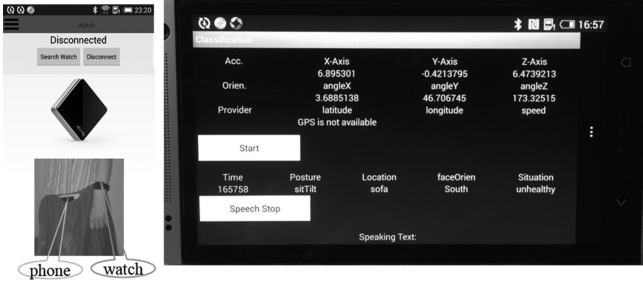
Fig. 8.   Interface of the situation-aware system on the phone. Top of the left figure is the phone connecting the watch when using it firstime; bottom of the left figure is a subject wearing the phone and watch at the same time. The right-hand side illustrates the user interface.

TABLE III
COMPARISON OF EXPERIMENTAL RESULTS FOR THREE TYPES OF FALLS WITH NORMAL LYING CLASSIFICATION, USING THE mulFusion AND accThresh ALGORITHMS, RESPECTIVELY

	mulFusion algorithm					*accThresh* algorithm				
	f-lyi.	f-sitT	p-fall	n-lyi.	total	f-lyi.	f-sitT	p-fall	n-lyi.	total
TP	122	119	9		250	126	0	9		135
FN	4	7	3		14	0	126	3		129
TN				72	72				0	0
FP				12	12				84	84
total	126	126	12	84	348	126	126	12	84	348
Positive predictive			95.4%					61.6%		
Negative predictive			83.7%					0%		
Sensitivity			94.7%					51.1%		
Specificity			85.7%					0%		

on a treadmill for 15 min first, get the heart rate is more than 90 bpm, then sit tilted on the sofa for a while.

5) Normal lying (**n-lyi**) approach1: From walk to sit on the bed for more than 2 s and then lying on the bed normally.

6) Normal lying (**n-lyi**) approach2: From walk to sit on the bed for less than 2 s, and then lying on the bed very quickly.

7) **Bend**: Do some bending (>30°) activity during the walking.

8) Sit tilted (**sitT**): Sit tilted right/left at the sofa for 6 min.

9) Sit still (**sitS**): Sit on a chair and watch television for 65 min.

Following these experiments, there were 126 f-lyi and 126 f-sitT in total (42 on the ground, 42 on the bed, 42 on the sofa); 12 p-fall in total (nine lying on the ground and three sit tilted on the sofa with higher heart rate); 42 normal lying using approach1; 42 normal lying using approach2; 101 Bend, 18 sitT, 18 sitS and a number of standing, walking, as well as sitting activities recorded and analyzed, indoors.

B. Outdoor Experiments

In the outdoor environment, each of the nine subjects walked from home to a park and then adopted the following postures: sit upright or sit back on the park bench for a period of time, and then walk around and bend two times during the walk; finally, sit on the bench again for a while. Thus, there were 18 normal sitting postures and 18 bend postures as well as a number of walking and stand activities recorded.

The outdoors localization was based on the coarse-grained subareas, for instance, GPS location may recognize the park area correctly, but it cannot recognize the bench area within the park. In this case, a possible fall can be raised if the user is sit tilted at the park (bench), since the system deems that the user is sit tilted on the *ground* outdoors.

C. Experimental Results

The postures data collected from the nine subjects were classified in real time and a voice reminder was delivered in real time. The interface of the system is shown in Fig. 8.

The experimental results based on the mulFusion algorithm are shown in Table II.

Table II demonstrates that the level of agreement is very good using the proposed mulFusion algorithm, since its Cohen's Kappa is 83.8%. For example, the accuracy of f-lyi and f-sitT detection were higher (96.8% and 94.4%, respectively). Some instances of f-lyi were classified as normal-lying when the user transitioned from walk to lying on the bed slowly, since in this case, the posture transition was recognized as from standing to lying, rather than from walk to lying.

The accuracy of possible falls (p-fall) classification was 75%. One of the 12 p-fall was classified as sit, since the ending "sit tilted" posture was recognized as sit. Another two of the 12 p-fall were classified as

normal lying, since the lying location ground was misclassified as bed (one of the three mats was located near to the bed). The accuracy of normal-lying (n-lyi) classification was 85.7%. Instances of of normal-lying were classified as f-lyi when the sitting period of time was less than 2 s before the normal lying, since in this case, the sitting posture was ignored, thus the posture transition was analyzed as from walk to lying directly. The accuracy of bend classification was lower (68.3%). Since the "deep waist bend" (more than 70°) has similar features (acceleration and phone's orientation angles) with lying when the phone was belt-worn on the waist, therefore, instances of bend were classified as f-lyi. In fact, bend classification accuracy is problematic, since it depends on dexterity and how much deep bending the users have done.

The classification accuracy for normal sit and stand were similar around 85%. Sit and stand were confused on occassion. The classification accuracy for unhealthy postures sit tilted (sitT) for more than 5 min and sit-still (sitS) for more than one hour all were 100%. For comparison, three types of falls with normal lying activity were classified using the mulThresh algorithm and accThresh algorithm, respectively. The experimental results (see Table III) were compared between both algorithms from four aspects: recognize real falls correctly (TP); recognize real falls as nonfall (FN); recognize nonfall activities correctly (TN); recognize nonfalls as a fall (FP).

Table III illustrates that the algorithm mulFusion can improve the falls detection accuracy and reliability significantly compared to the algorithm accThresh. The classification results for the three types of falls with normal lying, compared to accThresh, mulFusion had positive predictive value of 95.4% versus 61.6%, negative predictive value of 83.7% versus 0%, sensitivity of 94.7% versus 51.1%, and specificity of 85.7% versus 0%. The accThresh algorithm was able to detect all the falls ending with lying (f-lyi) correctly, nevertheless, it recognized 0/126 falls ending with sit tilted (f-sitT) and 0/84 of normal lying (n-lyi), since the normal lying posture also caused a large acceleration changing. For the 12 p-fall, it also only recognized the 9/12 correctly, which was ending with lying. Therefore, this threshold only algorithm was limited for the falls ending with sit-tilted situations.

In general the participants deemed the system helpful and easy to use. It is appareent that the "possible" fall music with a stop button can reduce the delivery of incorrect alerts.

V. CONCLUSION AND FUTURE WORK

The accuracy of falls detection algorithms reported in the literature is good. However, most of the accelerometer-based experiments involved typical falls with a high acceleration upon the impact with the ground.

Slow falls and normal lying are more difficult to detect. Fall-like events, which trigger false alarms, limit users' acceptance. The contribution of this paper is the development of a real-time situation-aware system for falls alert and unhealthy postures reminder, based on integrated multiple contexts (e.g., postures, transition, location, and heart rate) acquired from sensors embedded in a smartphone, in a smartwatch and using a deployed RFID network in an indoor environment.

Fall detection algorithms based on integrated multiple contexts can improve the accuracy of detection of certain falls distinguishing them from normal daily activities. Gjoreski *et al.* [17] studied a combination of body-worn inertial and location sensors for fall detection. They illustrated that the two types of sensors combined with context-based reasoning can significantly improve the performance. Compared to their study, this research combined four modalities (accelerometers, orientation, location, and heart rate). It is potentially more robust. This context-based work can be extended beyond determining falls. The postures sit tilted and sit still may, under certain circumstances, be defined as unhealthy postures. We know that back pain, neck pain, or shoulder pain can be avoided or managed by correcting posture; however, it can be difficult to maintain appropriate postures throughout the day. One of the most common causes of low back pain is poor sitting posture (e.g., sit tilted for a long time) [40]. Hence, it may be possible using this approach to remind people to correct poor postures in real time.

The accuracy of falls detection depends on the accuracy of posture classification and location detection. There are many sources of potential interference in a real living environment, such as electrical and magnetic interference (from electricity and fluorescent devices and even home-based networks). These are much harder to control than in a laboratory situation. In addition, there will be errors introduced by arte-fact, and absence of GPS signal outdoors. Such issues can be addressed in a longer study, once the technical feasibility, usability, and potential acceptance issues have been overcome or at least better understood. Services could be implemented in two ways: 1) alert can be delivered to caregivers immediately if a certain fall is detected; 2) music with a stop button can play if a possible fall is raised. A fall or a normal lying activity will be determined according to whether the user stops the alert music.

A study by van Hees *et al.* [41] has suggested that the classifier performance can be overestimated using controlled datasets. In future, we will study how to improve classification accuracy for an array of postures and transitions, and inferred situations in real-life conditions, especially for elderly at their home environments. In addition, smartphone-based solutions may have usability issues, since it is a re-quirement for the user to keep a smartphone at the fixed position [12]. As sensing technology continues to evolve, the use of a smartwatch for an additional channel of accelerometer data is worthy of further investigation. The phone can then be used for data analysis and reminders delivery, which may improve acceptance. The use of such technology for influencing longer term behavior change using real-time reminders requires further study of a longer period.

ACKNOWLEDGMENT

REFERENCES

[1] C. D. Nugent, M. D. Mulvenna, X. Hong, and S. Devlin, "Experiences in the development of a smart lab," *Int. J. Biomed. Eng. Technol.*, vol. 2, no. 4, pp. 319–331, 2009.

[2] J. Teno, D. P. Kiel, and V. Mor, "Multiple stumbles: A risk factor for falls in community-dwelling elderly," *J. Amer. Geriatrics Soc.*, vol. 38, no. 12, pp. 1321–1325, 1990.

[3] B. Najafi, K. Aminian, F. Loew, Y. Blanc, and P. A. Robert, "Measurement of stand-sit and sit-stand transitions using a miniature gyroscope and its application in fall risk evaluation in the elderly," *IEEE Trans. Biomed. Eng.*, vol. 49, no. 8, pp. 843–851, Aug. 2002.

[4] M. B. King and M. E. Tinetti, "Falls in community-dwelling older persons," *J. Amer. Geriatrics Soc.*, vol. 43, no. 10, pp. 1146–1154, 1995.

[5] G. Demiris and B. K. Hensel, "Technologies for an aging society: A systematic review of "smart home" applications," *Yearbook Med. Informat.*, vol. 3, pp. 33–40, 2008.

[6] H. Hawley-Hague and E. Boulton, "Older adults' perceptions of technologies aimed at falls prevention, detection or monitoring: A systematic review," *Int. J. Med. Informat.*, vol. 83, no. 6, pp. 416–426, 2014.

[7] A. Staranowicz, G. R. Brown, and G.-L. Mariottini, "Evaluating the accuracy of a mobile Kinect-based gait-monitoring system for fall prediction," presented at the 6th Int. Conf. Pervasive Technol. Related Assistive Environ., New York, NY, USA, 2013, Paper 57.

[8] U. Anliker *et al.*, "AMON: A wearable multiparameter medical monitoring and alert system," *IEEE Trans. Inf. Technol. Biomed.*, vol. 8, no. 4, pp. 415–427, Dec. 2004.

[9] *Fall Detector MCT-241MD PERS*, Visonic Inc., Tel Aviv, Israel, 2016. [Online]. Available: http://www.visonic.com/Products/Wireless-Emergency-Response-Systems/Fall-detector-mct-241md-pers-wer

[10] M. Kangas, A. Konttila, I. Winblad, and T. Jamsa, "Determination of simple thresholds for accelerometry-based parameters for fall detection," in *Proc. 29th Annu. Int. Conf. IEEE Eng. Med. Biol. Soc.*, 2007, pp. 1367–1370.

[11] U. Lindemann, A. Hock, M. Stuber, W. Keck, and C. Becker, "Evaluation of a fall detector based on accelerometers: A pilot study," *Med. Biol. Eng. Comput.*, vol. 43, no. 5, pp. 548–551, 2005.

[12] S. Abbate, M. Avvenuti, F. Bonatesta, and G. Cola, "A smartphone-based fall detection system," *Pervasive Mobile Comput.*, vol. 8, no. 6, pp. 883–899, 2012.

[13] J. T. Zhang, A. C. Novak, B. Brouwer, and Q. Li, "Concurrent validation of XSENS MVN measurement of lower limb joint angular kinematics," *Physiol. Meas.*, vol. 34, no. 8, pp. N63–N69, 2013.

[14] F. Bianchi, S. J. Redmond, M. R. Narayanan, S. Cerutti, and N. H. Lovell, "Barometric pressure and triaxial accelerometry-based falls event detection," *IEEE Trans. Neural Syst. Rehabil. Eng.*, vol. 18, no. 6, pp. 619–627, Dec. 2010.

[15] Q. Li, J. A. Stankovic, M. A. Hanson, A. T. Barth, J. Lach, and G. Zhou, "Accurate, fast fall detection using gyroscopes and accelerometer-derived posture information," in *Proc. 6th Int. Workshop Wearable Implantable Body Sensor Netw.*, Jun. 2009, pp. 138–143.

[16] M. Lustrek and B. Kaluza, "Fall detection and activity recognition with machine learning," *Informatica*, vol. 33, no. 2, pp. 197–204, 2009.

[17] H. Gjoreski, M. Gams, and M. Luštrek, "Context-based fall detection and activity recognition using inertial and location sensors," *J. Ambient Intell. Smart Environ.*, vol. 6, no. 4, pp. 419–433, 2014.

[18] N. Y. Ko and T. Y. Kuc, "Fusing range measurements from ultrasonic beacons and a laser range finder for localization of a mobile robot," *Sensors*, vol. 15, no. 5, pp. 11050–11075, 2015.

[19] T. Yamazaki, "Beyond the smart home," in *Proc. Int. Conf. Hybrid Inf. Technol.*, 2006, pp. 350–355.

[20] C. C. Hsu and P. C. Yuan, "The design and implementation of an intelligent deployment system for RFID readers," *Expert Syst. Appl.*, vol. 38, no. 8, pp. 10506–10517, 2011.

[21] J.-H. Seok, J.-Y. Lee, C. Oh, J.-J. Lee, and H. J. Lee, "RFID sensor deployment using differential evolution for indoor mobile robot localization," in *Proc. IEEE Int. Conf. Intell. Robots Syst.*, 2010, pp. 3719–3724.

[22] A. T. Murray, K. Kim, J. W. Davis, R. Machiraju, and R. E Parent, "Coverage optimization to support security monitoring," *Comput., Environ. Urban Syst.*, vol. 31, no. 2, pp. 133–147, 2007.

[23] F. Y. S. Lin and P. L. Chiu, "A simulated annealing algorithm for energy efficient sensor network design," in *Proc. 3rd Int. Symp. Model. Optim. Mobile, Ad Hoc, Wireless Netw.*, 2005, pp. 183–189.

[24] A. W. Reza and T. K. Geok, "Investigation of indoor location sensing via RFID reader network utilizing grid covering algorithm," *J. Wireless Pers. Commun.*, vol. 49, no. 1, pp. 67–80, 2009.

[25] J. Hightower, R. Want, and G. Borriello, "SpotON: An indoor 3D location sensing technology based on RF signal strength," Univ. Washington, Seattle, WA, USA, Tech. Rep. UW CSE 00-02-02, 2000.

[26] J. Zhou and J. Shi, "RFID localization algorithms and applications—A review," *J. Intell. Manuf.*, vol. 20, no. 6, pp. 695–707, 2009.

[27] K. Lorincz and M. Welsh, "MoteTrack: A robust, decentralized approach to RF-based location tracking," *Pers. Ubiquitous Comput.*, vol. 11, no. 6, pp. 489–503, 2007.

[28] X. Nguyen, M. I. Jordan, and B. Sinopoli, "A kernel-based learning approach to ad hoc sensor network localization," *ACM Trans. Sensor Netw.*, vol. 1, no. 1, pp. 134–152, 2005.

[29] L. M. Ni, Y. Liu, Y. C. Lau, and A. P. Patil, "LANDMARC: Indoor location sensing using active RFID," *Wireless Netw.*, vol. 10, no. 6, pp. 701–710, 2004.

[30] S. Zhang, P. McCullagh, J. Zhang, and T. Yu, "A smartphone based real-time daily activity monitoring system," *Cluster Comput.*, vol. 17, no. 3, pp. 711–721, 2014.

[31] S. Zhang, P. McCullagh, C. Nugent, H. Zheng, and N. Black, "A subarea mapping approach for indoor localisation," in *Toward Useful Services for Elderly and People With Disabilities*. Berlin, Germany: Springer-Verlag, 2011, pp. 80–87.

[32] S. Zhang, P. McCullagh, H. Zhou, Z. Wen, and Z. Xu, "RFID network deployment approaches for indoor localisation," in *Proc. 12th Int. Conf. Wearable Implantable Body Sensor Netw.*, Boston, MA, USA, 2015, pp. 1–6.

[33] C.-C. Chang and C.-J. Lin, "LIBSVM: A library for support vector machines," *ACM Trans. Intell. Syst. Technol.* vol. 2, no. 3, 2011, Art. no. 27. [Online]. Available: http://www.csie.ntuedu.tw/cjlin/libsvm

[34] S. Zhang, P. McCullagh, C. Nugent, H. Zheng, and M. Baumgarten, "Optimal model selection for posture recognition in home-based healthcare," *Int. J. Mach. Learn. Cybern.*, vol. 2, no. 1, pp. 1–14, 2011.

[35] Y. Kim, Y. Chon, and H. Cha, "Smartphone-based collaborative and autonomous radio fingerprinting," *IEEE Trans. Syst., Man, Cybern. C*, vol. 42, no. 1, pp. 112–122, Jan. 2012.

[36] S. Zhang, P. Mccullagh, C. Nugent, and H. Zheng, "Activity monitoring using a smart phone's accelerometer with hierarchical classification," in *Proc. 6th Int. Conf. Intell. Environ.*, 2010, pp. 158–163.

[37] S. Zhang, H. Li, P. McCullagh, C. Nugent, and H. Zheng, "A real-time falls detection system for elderly," in *Proc. 5th Comput. Sci. Electron. Eng. Conf.*, 2013, pp. 51–56.

[38] D. Zhang, X. Shen, and X. Qi, "Resting heart rate and all-cause and cardiovascular mortality in the general population: A meta-analysis," *Can. Med. Assoc. J.*, vol. 188, no. 3, pp. E53–E63, 2016.

[39] S. Zhang, P. McCullagh, C. Nugent, and H. Zheng, "A theoretic algorithm for fall and motionless detection," in *Proc. 3rd Int. Conf. Pervasive Comput. Technol. Healthcare*, 2009, pp. 1–6.

[40] P. J. Mork and R. H. Westgaard, "Back posture and low back muscle activity in female computer workers: A field study," *Clin. Biomech.*, vol. 24, no. 2, pp. 169–175, 2009.

[41] V. T. van Hees, R. Golubic, U. Ekelund, and S. Brage, "Impact of study design on development and evaluation of an activity-type classifier," *J. Appl. Physiol.*, vol. 114, no. 8, pp. 1042–1051, 2013.